

# Simulation of the Influence of Loading Fraction on Operational Shipping Fuel Consumption and Emissions

**Wei Shi** (MSc, Delft University of Technology)

**Prof. D. Stapersma** (MSc, FIMarEST, CEng, Professor of Marine Engineering, Delft University of Technology  
/Netherlands Defense Academy)

**Dr. H.T. Grimmelius** (PhD, MSc, BSc, MIMarEST, CEng, Delft University of Technology)

*Simulation methodology is used to assess the influence of loading fraction on operational shipping fuel consumption and emissions. By means of mathematical analysis and computer model simulation, the effect of loading fraction on both propulsion and auxiliary systems is demonstrated. The paper presents quantitative and qualitative results of the effects on fuel consumption and CO<sub>2</sub>, SO<sub>2</sub> emissions, for different types of ships at both design and off-design speed. The paper shows that neglecting the influence of loading fraction would result in remarkable errors in the prediction of fuel consumption and a serious misestimate of emissions.*

## KEY WORDS

Loading fraction; Fuel consumption; Exhaust emissions

## NOMENCLATURE

$A_{ship}$	wetted surface of the hull	[m <sup>2</sup> ]	$P_{reefer}$	cargo auxiliary power per reefer	[kW]
$C_b$	block coefficient at moulded draft $T_m$		$P_{trans}$	delivered power in transmission system	[kW]
$C_b'$	block coefficient at draft $T$		$Q_{prop}$	torque of the propeller	[Nm]
$C_E$	non-dimensional specific resistance factor		$R_A$	model-ship correlation resistance	[N]
$C_Q^*$	thrust coefficient		$R_{app}$	resistance of appendages	[N]
$C_{R^*}$	non-dimensional resistance factor		$R_B$	additional pressure resistance of bulbous bow near the water surface	[N]
$C_T$	torque coefficient		$R_F$	frictional resistance according to the ITTC-1957 friction formula	[N]
$D_{prop}$	diameter of propeller,	[m]	$R_{ship}$	total resistance of ship	[N]
$DWT_{full}$	full deadweight of ship	[ton]	$R_{TR}$	additional pressure resistance of immersed transom stern	[N]
$LHV_{fuel}$	lower heating value of the fuel	[kJ/kg]	$R_w$	wave-making and wave-breaking resistance	[N]
$L_{wl}$	water line length of the ship	[m]	$T$	actual draft of the ship	[m]
$M_{(i)}$	moment of each particular propulsion component, such as the propeller, the shaft, the gearbox and the engine	[kNm]	$T_m$	moulded draft of the ship	[m]
$N_{person}$	number of the person on board		$T_{prop}$	thrust of the propeller	[N]
$N_{reefer}$	number of the reefer in operation		$V_A$	advance speed	[m/s]
$P_{a\_cargo}$	cargo auxiliary power	[kW]	$V_{ship}$	sailing speed of the ship	[knot]
$P_{a\_me}$	main engine auxiliary power	[kW]	$k_{l+1}$	form factor describing the viscous resistance of the hull form in relation of $R_F$	
$P_B$	engine brake power	[kW]	$\dot{m}_{fuel}$	fuel consumption	[kg/hr]
$P_{B\_ae}$	brake power of auxiliary engine	[kW]	$\dot{m}_{fuel\_me}$	fuel consumption of main engine	[kg/hr]
$P_{B\_me}$	brake power of main engine	[kW]	$m_{max}$	maximum loading mass of ship	[ton]
$P_E$	effective towing power	[kW]	$m_{payload}$	mass of payload	[ton]
$P_{hotel}$	hotel power	[kW]	$m_{se}$	mile specific energy consumption	[kWh/mile]
$P_{i\_me}$	installed power of main engine	[kW]	$msfc$	mile specific fuel consumption	[g/mile]
$P_{loss}$	lost power in transmission system,	[kW]	$n_{(i)}$	rotation speed of each particular propulsion component, such as the propeller, the shaft, the gearbox and the engine	[rad/s]
$P_{person}$	hotel power per person on board	[kW]	$sfc$	power specific fuel consumption	[g/kWh]
			$tmsfc$	ton-mile specific fuel consumption	[g/ton-mile]

$x$	actual loading fraction, the ratio between the mass of actual and maximum payload	
$x_b$	benefit loading fraction, the ratio between the mass of transport cargo and the maximum payload	
$y$	ratio between maximum payload and full deadweight	
$z$	ratio between full deadweight and full mass displacement	
$\Delta$	mass displacement of the ship	[ton]
$\Delta_{full}$	full mass displacement of the ship	[ton]
$\Delta_{light}$	light mass displacement of the ship	[ton]
$\beta$	advance angle at 70% radius	[°]
$\eta_{ae}$	efficiency of the auxiliary engine operation	
$\eta_{DRTR}$	overall efficiency of the drive train (containing the propeller efficiency hull/propeller interaction and transmission losses)	
$\eta_{me}$	efficiency of the main engine operation	
$\rho$	seawater density	[kg/m <sup>3</sup> ]
$()^*$	relative quality	

## INTRODUCTION

In analysis of operational shipping activities, the general practice is to set the ship loading fraction as 100%, which represents full load. But, for most merchant ships, this is rarely the case, due to the maritime logistic system and issues of ship stability. For a container ship, a more sensible estimation is such, that the larger the ship, the higher loading fraction it has, because of its better logistical networking. For a bulk carrier, the average loading fraction for a particular route is about 0.5, since it sails half of the journey with ballast water. For a ferry, due to its commercial profile and the large fluctuation of the amount of cargo or the number of passengers, the variability of loading fraction can be significant.

To be able to model a realistic operational profile, the total required energy is split into two parts: the propulsion energy and the auxiliary energy. Furthermore the auxiliary energy can be subdivided into the auxiliary operational energy and the cargo handling energy. The requirements of both the propulsion energy and the cargo handling energy are related to loading conditions – the amount and the character of the payload, but few studies have been conducted on the influence of the loading fraction on operational shipping activities.

This paper focuses on the fuel consumption and engine exhaust emissions (CO<sub>2</sub> and SO<sub>2</sub>) in off-design conditions – part load of the ship and low speed operation. Different types of ships, including container ship, bulk carrier and cargo/passenger ferry, are involved. To demonstrate the influence on both the propulsion energy requirement and the auxiliary energy requirement in these off-design conditions, a series of operational shipping activities are investigated by means of computer simulation.

## MATHEMATICAL ANALYSIS

Considering the commonly used g/kWh unit for judging operational shipping activities, a more logical approach to quantification of the fuel consumption and exhaust emissions from ships in a particular voyage is to involve not only the energy consumption but also the covered distances and the

transferred cargo. This leads to the so called ton-mile specific factors. To convert ton-mile specific factors from power specific factors, as illustrated in Fig. 1, starting from the power specific factors in unit of g/kWh, by combining the ship resistance and propulsion efficiency, the mile specific factors can be expressed in the unit of g/mile. One step further, after dividing the mile specific factors by the amount of payload of the ship, the results are ton-mile specific factors. Furthermore, if the emission ratio for the selected fuel is brought into this chain, the results could be ton-mile specific pollutant emissions.

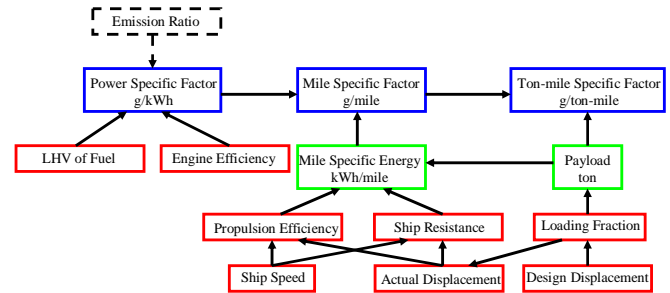


**Fig. 1 Units of expressing ship activities and required data for a ship system (Stapersma, 2003)**

Writing each part of the chain in mathematical equations, one gets eqs. 1~4 to express the fuel consumption, when sailing at sea:

$$sfc_i = \frac{1000\dot{m}_{fuel,i}}{P_{B,i}} \quad (1)$$

$$mse_i = \frac{P_{B,i}}{V_{ship}} \quad (2)$$

$$msfc = \sum (sfc_i \cdot mse_i) \quad (3)$$

$$tmsfc = \frac{msfc}{m_{payload}} = \frac{\sum \dot{m}_{fuel,i}}{m_{payload} \cdot V_{ship}} \quad (4)$$

The subscript  $i$  represents each individual engine.

In this paper, the loading fraction  $x$  and the maximum payload fraction  $y$  are defined to estimate the mass of the payload, shown in eqs. 5~6.

$$x = \frac{m_{payload}}{m_{max}} \quad (5)$$

$$y = \frac{m_{max}}{DWT_{full}} \quad (6)$$

Thus the mass of the payload is related to a ship design parameter, the full deadweight tonnage ( $DWT_{full}$ ), which indicates the cargo capacity of the ship and is the common parameter to indicate the size of cargo ships.

With the known information of these two factors, the mass of payload can be calculated by:

$$m_{payload} = xyDWT_{full} \quad (7)$$

When looking from the power supply side, the fuel consumption can be generally calculated by using:

$$\dot{m}_{fuel} = \frac{3600P_B}{LHV_{fuel} \cdot \eta_{engine}} \quad (8)$$

Then, putting together the chain from fuel flow to ton-mile specific fuel consumption as shown in Fig. 1, this results in the following equation for the ton-mile specific fuel consumption:

$$tmsfc = \frac{3.6 \cdot 10^6 \cdot P_B}{LHV_{fuel} \cdot \eta_{engine}} / m_{payload} / V_{ship} \quad (9)$$

$$= \left( \frac{3.6 \cdot 10^6 \cdot P_B}{LHV_{fuel} \cdot \eta_{engine}} \right) \cdot \left( \frac{1}{xy \cdot DWT_{full}} \right) \cdot \left( \frac{1}{V_{ship}} \right)$$

## Analysis of Propulsion System

It is of importance to look at the power transmission through the propulsion system, from the engine brake power to the effective towing power, following (Klein Woud, 2002). The whole power chain can be broken down into 6 parts, as shown in Fig. 2:

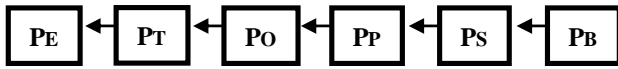


Fig. 2 Power chain of propulsion system

With:

$$\text{Engine brake power: } P_B = 2\pi \cdot M_{engine} \cdot n_{engine} \quad (10)$$

$$\text{Shaft power: } P_S = 2\pi \cdot M_{shaft} \cdot n_{shaft} \quad (11)$$

$$\text{Propeller power: } P_P = 2\pi \cdot M_{prop} \cdot n_{prop} \quad (12)$$

$$\text{Open water propeller power: } P_O = 2\pi \cdot Q_{prop} \cdot n_{prop} \quad (13)$$

$$\text{Thrust power: } P_T = T_{thrust} \cdot V_{advance} \quad (14)$$

Then, a series of coefficient are defined:

$$\text{Hull efficiency: } \eta_H = P_E / P_T \quad (15)$$

$$\text{Open water efficiency: } \eta_O = P_T / P_O \quad (16)$$

$$\text{Relative rotative efficiency: } \eta_R = P_O / P_P \quad (17)$$

$$\text{Shaft efficiency: } \eta_S = P_P / P_S \quad (18)$$

$$\text{Gearbox efficiency: } \eta_{GB} = P_S / P_B \quad (19)$$

By combining eqs. 15~19, the drive-train efficiency is:

$$\eta_{DRTR} = \eta_H \eta_O \eta_R \eta_S \eta_{GB} \quad (20)$$

From the power demand side, the main engine brake power can be expressed as:

$$P_{B\_me} = P_E / \eta_{DRTR} \quad (21)$$

Therefore, the ton-mile specific fuel consumption for the propulsion system is:

$$tmsfc_{propul\_system} = \left( \frac{3.6 \cdot 10^6}{LHV_{fuel} \cdot \eta_{me}} \right) \cdot \left( \frac{P_E}{\eta_{DRTR}} \right) \cdot \left( \frac{1}{xy \cdot DWT_{full}} \right) \cdot \left( \frac{1}{V_{ship}} \right) \quad (22)$$

In order to propel the ship at a specified speed, the thrust developed by the propulsion system has to overcome the resistance of the ship. The general mathematical expression from the power demand side is:

$$P_E = \left( \frac{R_{ship}}{1000} \right) \cdot \left( \frac{1852}{3600} V_{ship} \right) = \frac{1852}{3.6 \cdot 10^6} (R_{ship} V_{ship}) \quad (23)$$

In hydrodynamics, the total resistance  $R_{ship}$  is usually written in non-dimensional form as  $C_R$ :

$$C_R = \frac{R_{ship}}{0.5 \cdot \rho \cdot A_{ship} \cdot \left( \frac{1852}{3600} V_{ship} \right)^2} \quad (24)$$

However, the wetted surface is not always easily available. Therefore, in (Klein Woud, 2002), a non-dimensional factor  $C_E$  is defined to analyze the effective towing power,  $P_E$ , based on the displacement:

$$C_E = \frac{1000P_E}{\rho^{1/3} (1000\Delta)^{2/3} \left( \frac{1852}{3600} V_{ship} \right)^3} \quad (25)$$

Besides the factors  $x$  and  $y$ , another factor  $z$  is defined in this paper to take into account the difference between the full deadweight and the full mass displacement of the ship:

$$z = \frac{DWT_{full}}{\Delta_{full}} \quad (26)$$

The mass displacement of ship can be divided into two parts:

$$\Delta = \Delta_{light} + m_{payload} \quad (27)$$

$$\Delta_{light} = \Delta_{full} - m_{max} \quad (28)$$

Then, by combining the eqs. 5~6 and eqs. 26~28, the actual mass displacement of the ship can be calculated:

$$\Delta = \frac{(1 - yz + xyz)}{z} DWT_{full} \quad (29)$$

Thus, by combining eq. 25 and eq. 29 into eq. 22, the following "master" equation of ton-mile specific fuel consumption of propulsion system is derived:

$$\begin{aligned}
tmsfc_{propul\_system} &= 49013.75 \\
&\cdot \left(\frac{1}{LHV_{fuel}}\right)_{fuel} \\
&\cdot \left(\frac{1}{\eta_{me}}\right)_{engine} \\
&\cdot \left(\frac{C_E \cdot \rho^{1/3}}{\eta_{DRTR} \cdot DWT_{full}^{1/3}}\right)_{ship} \\
&\cdot \left(\frac{(1-yz+xyz)^{2/3}}{xyz^{2/3}} \cdot V_{ship}^2\right)_{operation}
\end{aligned} \quad (30)$$

In this master equation the ton-mile specific fuel consumption of propulsion system is related to a wide range of factors belonging to four segments:

1. The fuel property (lower heating value).
2. The engine operational condition (engine efficiency).
3. The ship (specific resistance, drive train efficiency and full deadweight tonnage).
4. The ship voyage profile (cargo capacity and ship speed).

### Analysis of Auxiliary System

In general, the required power of the auxiliary systems of the ship consists of three parts: the main engine auxiliary power, the cargo auxiliary power and the hotel power. The following expression is used in this paper.

$$P_{B\_ae} = P_{a\_me} + P_{a\_cargo} + P_{hotel} \quad (31)$$

Then, insert the eq. 31 into the eq. 9, the “master” equation of ton-mile specific fuel consumption of the auxiliary system is:

$$\begin{aligned}
tmsfc_{aux\_system} &= 3.6 \cdot 10^6 \\
&\cdot \left(\frac{1}{LHV_{fuel}}\right)_{fuel} \\
&\cdot \left(\frac{1}{\eta_{ae}}\right)_{engine} \\
&\cdot (P_{a\_me} + P_{a\_cargo} + P_{hotel})_{auxiliary\_system} \\
&\cdot \left(\frac{1}{xy \cdot DWT_{full} \cdot V_{ship}}\right)_{operation}
\end{aligned} \quad (32)$$

The engine auxiliary power and hotel power can be simply calculated by using the eq. 33~34, refer to (Stapersma, 2003).

$$P_{a\_me} = 100 + 0.55 \cdot P_{i\_me}^{0.6} \quad (33)$$

$$P_{hotel} = N_{person} \cdot P_{person} \quad (34)$$

It should be noted that eq. 33 applies to use the installed propulsion power to determine the electric power demand in operating main engines at sea for a conventional cargo vessel. However, in this paper, as the first estimation, this formula is

also used to calculate the main engine auxiliary power of other types of ships.

When considering the different kinds of ships (see APPENDIX), the contribution of the components in eq. 31 would be different too, in particular for the cargo auxiliary power.

**Container ship.** Container ships are cargo ships that carry all load in containers. In order to transport perishable commodities, such as fruits, meat, fish, vegetables, dairy products and other food, a temperature-controlled transportation is required. So, in modern container ships, there are some plugs for refrigerated containers (reefers), but the amount of reefers a ship can carry is limited due to the lack reefer connections and insufficient generator capacity. Therefore the main issue, which would influence the cargo auxiliary power of a container ship, is the type of the cargo the container ship transports. For normal containers, no extra power is needed, but the connected reefers require electric power to maintain the inside temperature and the energy requirement is growing with the number of the connected reefers. Then the expression of cargo auxiliary power of a container ship should be:

$$P_{a\_cargo} = N_{reefer} \cdot P_{reefer} \quad (35)$$

Table 1 gives the container capacities of the reference container ships (Ship 1 ~ Ship 4).

**Table 1. Container capacity and reefer plugs**

	Container capacity	Reefer plugs	Percentage of reefer
Ship 1	6802	660	9,7%
Ship 2	2046	990	48,4%
Ship 3	1122	150	13,4%
Ship 4	344	50	14,5%

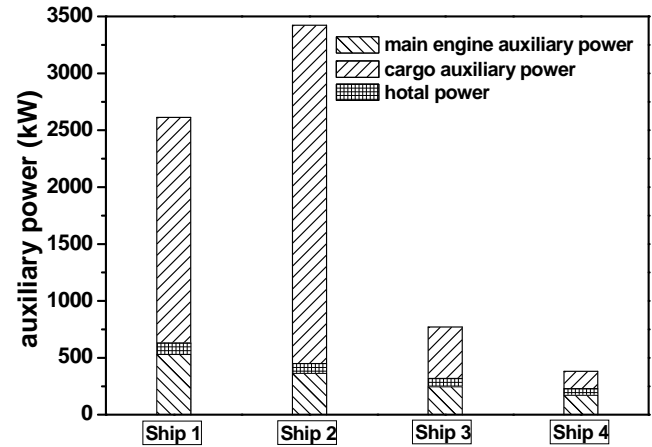


**Fig. 3 Components of auxiliary power of container ships**

In this paper, for the reference container ships, the assumptions are:

$$P_{reefer} = 3\text{kW}$$

$$P_{person} = 3\text{kW}$$

- $N_{person} = 20$  (for Ship 1: large container ship)  
 18 (for Ship 2: medium container ship)  
 16 (for Ship 3: container feeder)  
 14 (for Ship 4: coast feeder)

The contributions of each part of auxiliary system on the power requirement are shown in Fig. 3. As illustrated in Fig. 3, the cargo auxiliary power requirement dominates the picture. The main engine auxiliary power requirement and hotel power requirement are determined by the size of the container ship and would remain constant during the particular voyage. In general, the larger the container ship, the more electric energy is required to support the main engine operation and the hotel facilities. On the other hand, the cargo auxiliary power requirement is very flexible. This part of energy requirement could have a wide range from 0 to over 8 times of the total of the other two parts (the case of Ship 2).

**Bulk Carrier.** Bulk carriers are merchant ships specially designed to transport unpackaged bulk cargo, such as grains, coal, ore and cement in its cargo holds. In this paper only the cruising part of the voyage is considered, so the energy required for loading and unloading is excluded and the cargo handling energy is judged as negligible. No extra power is needed to maintain cargo for the reference bulk carriers – the dry bulk carriers. Then, the auxiliary energy requirement for a particular reference bulk carrier is constant:

$$P_{B\_ae} = P_{a\_me} + P_{hotel} \quad (36)$$

For Ship 5 (large bulk carrier), the number of the crew is chosen as 16, and 14 for Ship 6 (medium size bulk carrier) and the hotel power per person on board is also set as 3kW.

**Cargo/passenger Ferry.** Ferries form a part of the public transport systems of waterside cities and islands, and most of them operate on regular, frequent, return services. A cargo/passenger ferry usually operates in a short distance, i.e. directly transit between points and with many stops between points. Normally, the cargo handling power can be neglected.

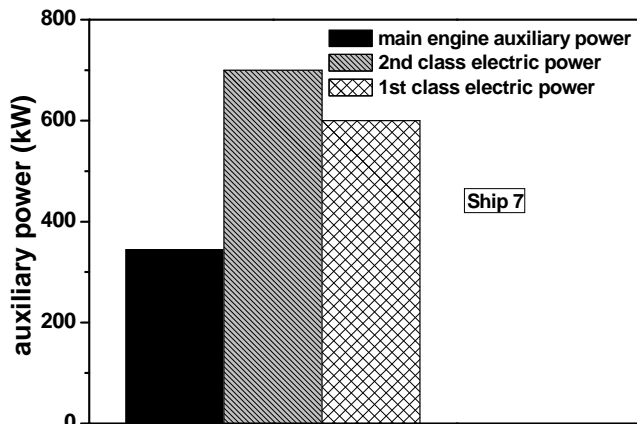


Fig. 4 Components of auxiliary power of ferry

However, different from container ships and bulk carriers, the cargo/passenger ferries consume more electric energy for the hotel load, since they also transport passengers. The requirement of electric power is to satisfy passengers' comfort, and mainly depends on the passengers' requirement. In the reference ferry, two kinds of comfort classes are included:

- 1<sup>st</sup> class: 10kW electric power per passenger is needed and occupies 30% of the total passenger capacity.
- 2<sup>nd</sup> class: 6kW electric power per passenger is needed and occupies 70% of the total passenger capacity.

The power requirements are shown in Fig. 4.

## Loading Fraction

Referring to the master equations (eq. 30 and eq. 32), the weight factors  $x$ ,  $y$  and  $z$  indicate the actual loading condition of ships, and accordingly influence the ton-mile specific fuel consumption and the exhaust emissions.

For each of the reference ships, the factor  $z$  is taken as a constant per ship and the factor  $y$  can be calculated from the amount of fuel, by neglecting the fuel consumption during the voyage. The values of  $y$ ,  $z$  of reference ships are presented in Table 2.

Table 2. Weight factors of reference ships

	$Displ_{full}$ (ton)	$DWT_{full}$ (ton)	Fuel consumption (ton)	$y$	$z$
Ship 1	111825	83826	12835	0.85	0.75
Ship 2	42540	30560	4700	0.85	0.72
Ship 3	18903	11870	1761	0.85	0.63
Ship 4	5585	3820	273	0.93	0.68
Ship 5	179250	156300	5310	0.97	0.87
Ship 6	52559	44579	1919	0.96	0.85
Ship 7	16903	5640	980	0.83	0.33

As defined previously, the loading fraction  $x$  is the ratio between the actual and maximum amount of payload. But with regard to the real operation conditions, the mass displacement of ship changes less than the payload, from full load to empty load, since in empty load condition, due to stability reason, ballast is taken on board. In this paper the payload is subdivided into two parts: the cargo (the benefit) and the ballast water (the penalty). Then, the amount of benefit payload should be expressed as:

$$m_{payload\_b} = x_b \cdot y \cdot DWT_{full} \quad (37)$$

Table 3. Loading capacities of reference ships

	Max. Payload (ton)	Ballast Capacity (ton)
Ship 1	70991	20400
Ship 2	25860	12000
Ship 3	10109	4743
Ship 4	3547	2110
Ship 5	150900	19300
Ship 6	42660	9000
Ship 7	4660	2800

Table 3 presents the cargo capacities and ballast water capacities of the reference ships and Fig. 5 illustrates the relationship between the benefit loading fraction ( $x_b$ ) and the actual loading fraction ( $x$ ).

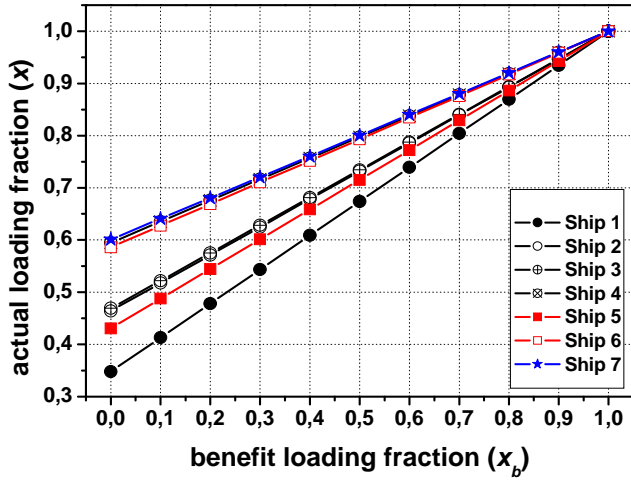


Fig. 5 Correction of benefit loading fraction

In this paper, all the results are generated by using the actual loading fraction  $x$ , (the actual operation condition), and presented corresponding to the benefit loading fraction  $x_b$ .

## COMPUTER SIMULATION

### Simulation Model

A simulation model is built in Matlab Simulink® to estimate propulsion activities. The block diagram is shown in Fig. 6.

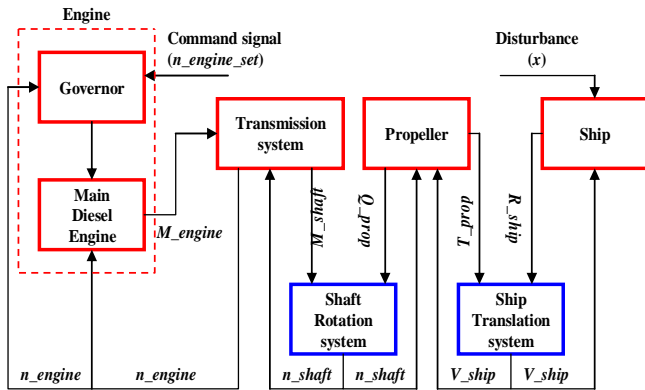


Fig. 6 Propulsion system of simulation model

The propulsion system model describes the dynamics of the ship propulsion plant by combining the models of four subsystems: a diesel engine & governor model, a transmission system model, a propeller model and a ship hydrodynamic force model. These four models are connected through two dynamic systems: a shaft rotation system and a ship translation system.

In this study the command signal of the model is the engine speed ( $n_{engine\_set}$ ), which determines the ship speed. Another input is the actual loading fraction ( $x$ ), which disturbs the ship resistance. The output data would be the corresponding fuel consumption and engine exhaust emissions.

Referring to the propulsion chain shown in Fig. 2,  $P_E$ ,  $P_T$  and  $P_O$  will be directly influenced by the loading fraction in cruising operation conditions, in other words, a different loading fraction will cause a different ship resistance, wake factor and thrust deduction factor, as well as a different propeller performance. Then, the result is a different engine brake power, fuel consumption and also different engine exhaust emissions.

**Ship Resistance.** In the ship design phase, there are different kinds of methods (Taylor, 1943; Moor, 1968; Holtrop, 1978; Holtrop, 1982) to predict ship resistance and other factors, on the basis of ship dimensional parameters. In this paper, the Holtrop and Mennen method is used to calculate ship resistance in both design and off-design conditions.

The total ship resistance can be divided into six parts:

$$R_{total} = (k_1 + 1)R_F + R_{APP} + R_w + R_B + R_{TR} + R_A \quad (38)$$

With a series of formulas given in (Holtrop, 1978; Holtrop, 1982), acceptable results of ship resistance can be calculated for all of the reference ships. But, in off-design conditions, (part load of ship), the parameters used in these formulas must be taken slightly different from those used in design condition, (full load of ship), i.e. the  $L_{wl}$  and  $C_b$  will change along with the loading fraction, and of course the draft,  $T$ .

In this study, due to the lack of body shape data of the reference ships, in off-design conditions, some assumptions are made:

1.  $L_{wl}$  is considered constant.
2. The draft ( $T$ ) changes linearly with the ship displacement.
3. An amendment for the body coefficient  $C_b$  in part load condition is implemented using a relationship between  $C_b$  at the moulded draft ( $T_m$ ) and  $C_b'$  at a draft  $T$  given by (Watson, 1998):

$$C_b' = C_b \left[ 1 + \frac{(1 - C_b)(1 - \frac{T_m}{T})}{3C_b \cdot \frac{T_m}{T}} \right] \quad (39)$$

4. Changes of other parameters are neglected.

**Propeller Performance.** In the propeller model, the Wageningen B-Screw Series are used to predict the propeller thrust and the generated torque. The four quadrant methodology proposed in (Kuiper, 1992) is applied in this paper, using eqs. 40~42:

$$\beta = \arctan\left(\frac{V_A}{0.7\pi \cdot n_{prop} \cdot D_{prop}}\right) \quad (40)$$

$$C_T^* = \frac{T_{prop}}{\frac{1}{2} \rho \cdot (V_A^2 + (0.7\pi \cdot n_{prop} \cdot D_{prop})^2) \cdot \frac{\pi}{4} \cdot D_{prop}^2} \quad (41)$$

$$C_Q^* = \frac{Q_{prop}}{\frac{1}{2} \rho \cdot (V_A^2 + (0.7\pi \cdot n_{prop} \cdot D_{prop})^2) \cdot \frac{\pi}{4} \cdot D_{prop}^3} \quad (42)$$

In order to implement the four quadrants diagrams, propeller data are generated using the model developed by (Roddy, 2006). These are introduced in the computer simulation model as two lookup tables. One translates the calculated parameter  $\beta$  to  $C_T^*$  and the other translates  $\beta$  to  $C_Q^*$ . Thus, the propeller thrust and delivered torque in every simulation time step can be determined. When calculating  $V_A$  from ship speed the effective wake factor according to (Holtrop, 1982) is used. The same source gives values for the thrust deduction factor and relative rotative efficiency, that are used to correct the open water thrust  $T_{prop}$  and torque  $Q_{prop}$ .

**Transmission System.** Along the chain from main engines to propellers, the transmission losses are taken into account. Generally, these mechanic losses are broken down into gearbox losses and shaft losses.

For both the gearbox and the shaft losses it is assumed that a part is proportional to the transmitted power, another part is proportional to the transmitted torque and that the balance is proportional to shaft speed, refer to (Stapersma, 1994). In the simulation model the gearbox losses and shaft losses are expressed as:

$$P_{loss}^* = k_1 P_{trans}^* + k_2 M_{trans}^* + k_3 n_{trans}^* \quad (43)$$

According to the author's experience, the coefficients ( $k_1$ ,  $k_2$ ,  $k_3$ ) are chosen as 0.5, 0.4, and 0.1, for estimating both gearbox losses and shaft losses.

**Diesel Engine Model.** A simplified calculation method is used to predict engine output torque on the basis of engine speed and the injected fuel per cycle. As a variation to (Brussen, 2006), the algorithm can be expressed as:

$$M_{engine}^* = 1 - a(1 - n_{engine}^*) + b(1 - n_{engine}^*)^2 - c(1 - \dot{m}_{fuel\_me}^*) + d(1 - \dot{m}_{fuel\_me}^*)^2 + 2e(1 - n_{engine}^*)(1 - \dot{m}_{fuel\_me}^*) \quad (44)$$

According to eq. 44, there are five parameters which determine the trend of engine output torque. Typical values of these parameters are given in Table 4.

**Table 4. Parameters for engine torque prediction**

$n_{engine}^*$	$\dot{m}_{fuel}^*$	$M_{engine}^*$
1	0.5	0.48
1	0.06	0
0.75	0.5	0.49
0.5	0.25	0.2
0.5	0.04	0

With all of the parameters known, the numerical values of engine fuel consumption and engine output torque can be predicted with this diesel engine model.

## SIMULATION RESULTS

### Power Requirement

**Power Requirement of Propulsion System** In the previous section, it has been shown that, the propulsion power will be different in various loading conditions, because of the change of the ship resistance. By means of computer simulations of the propulsion system, the relationship between loading conditions and main engine operation conditions are achieved, see Fig. 7 as an example. Fig. 7 illustrates the relative main engine brake power for reference ships, while carrying different amount of cargoes or passengers, operating at their service speeds. In order to make the results comparable, the relative values are plotted by choosing the main engine brake power in full load conditions as 85% MCR, which indicates the normal engine operation when sailing at sea. Bear in mind that, in the simulation process, the conversion is made between loading fraction ( $x$ ) and benefit loading fraction ( $x_b$ ), on the basis of Fig. 5. Typically, the same trends are also found at off-design speeds.

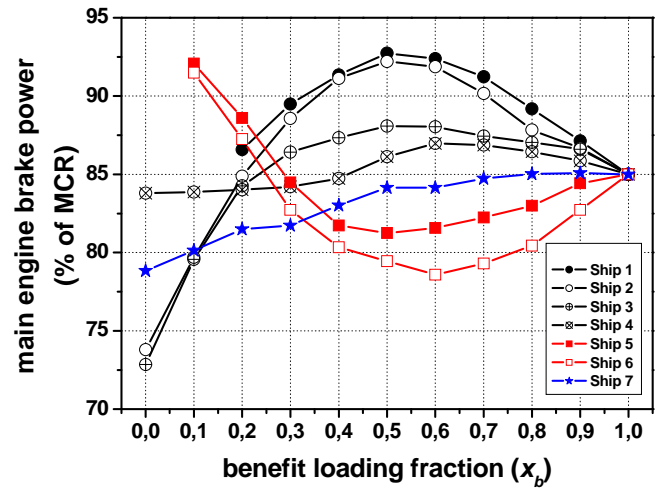


**Fig. 7 Relative engine brake power of reference ships at service speed**

The curves in Fig. 7 show that, the fluctuations of the requirements of main engine brake power in part load conditions are within 20% of MCR.

For cargo ships, comparing the larger ones (Ship 1, 2, 3, 5, 6) with the smaller one (Ship 4), Fig. 7 illustrates that, when sailing at their service speeds, the gaps of propulsion power requirements between full load condition and part load condition for the larger ones are bigger than that for the smaller one, because of their smaller amounts of ballast water compare to their deadweights. Also there are reversed trends between container ships and bulk carriers. Because of the different operational purposes and design concepts of the ship hull form, the conclusion is that, by decreasing the benefit loading fraction, the required main engine brake power of container ships first increases and then decreases, while the reverse trend applies to bulk carriers.

In this study, the size of Ship 7 (ferry) is comparable to the larger cargo ships, but the difference of required propulsion power between full load and part load conditions is only about 7%, which is relatively smaller than those of large cargo ships. The reason is that the ratio between deadweight and full mass displacement (factor  $z$ ) of a ferry is much smaller than that of a large cargo ship. Then, in different loading conditions, the mass displacement of the ferry only slightly changes, resulting in limited changes of ship resistance, which in turn lead to a small difference of main engine brake power.

According to the ‘master’ equation, eq. 30, the propulsion power also depends on the sailing speed of the ship. Another kind of off-design operational condition – the low speed operation– is considered to be superimposed on the effect of loading fraction. Only the results of Ship 1 (large container ship) are presented as an example, but the conclusions also apply to the other reference ships.

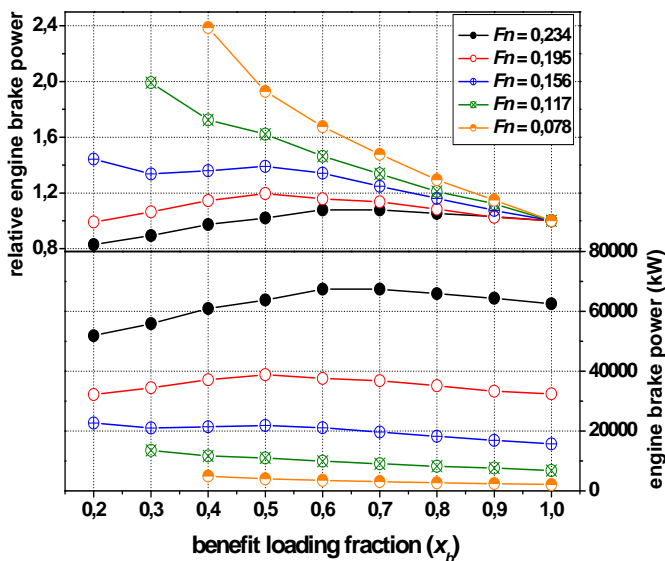


Fig. 8 Engine brake power of Ship 1 at variable speed

As shown in Fig. 8, when sailing at low speed, the propulsion power is much lower than at high speed. At each sailing speed, the propulsion power of course also changes along with the loading conditions.

Looking at the relative values, the engine brake power in full load conditions is set as 100% for each sailing speed. It is evident that the gaps in main engine brake power between full load conditions and part load conditions increase with decreasing sailing speed. For Ship 1 (large container ship), in 40% benefit loading condition, the gap is about 5% at service speed ( $Fn = 0.234$ ), while at low speed ( $Fn = 0.078$ ), the power requirement is almost 2.5 times of that in the corresponding full load condition.

## Fuel Consumption

It should be noted that for some of the reference ships (Ship 1, 2, 3, 4, 6), different fuel oils are used in main engines and auxiliary engines (See APPENDIX). The fuel properties are:

HFO (Heavy Fuel Oil), LHV = 40,000 kJ/kg, with a carbon content of 84% and a sulfur content of 3.5% on mass basis.

MDO (Marine Diesel Oil), LHV = 42,700 kJ/kg, with a carbon content of 86% and a sulfur content of 0.5% on mass basis.

In this paper the MDO consumptions are corrected to HFO consumptions.

**Amount of Fuel Consumption.** On the basis of the analysis of the influence of loading fraction on propulsion power requirement and auxiliary power requirement in the previous sections, the results of fuel consumption are presented. In this section, the Ship 2 (medium container ship) is chosen as an example to analyze the influence of loading fraction on fuel consumptions of both propulsion system and auxiliary system.

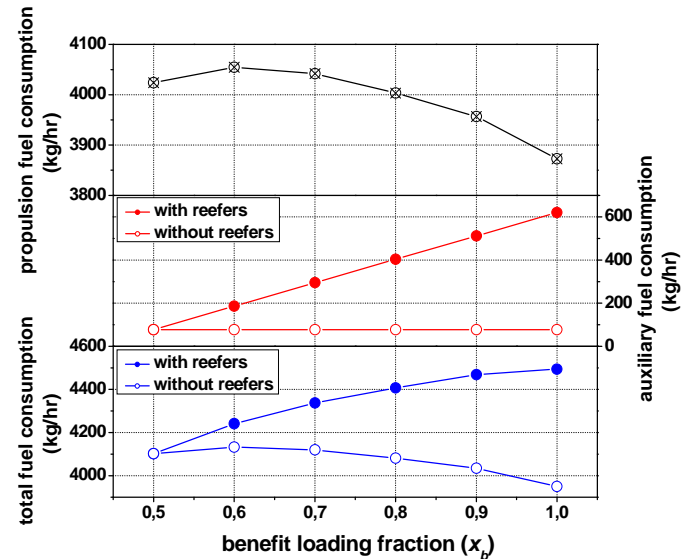


Fig. 9 Fuel consumptions of Ship 2 at service speed

Fig. 9 shows the fuel consumption of Ship 2 (medium container ship), when sailing at its service speed. As illustrated in this figure, the fuel consumption of the propulsion system has the same trend as the engine brake power, shown in Fig. 7: the fuel consumption increases while the loading weight decreases, until, after reaching the highest value at 60% benefit loading, it goes down. For the auxiliary system, the fuel consumption is mainly determined by the number of connected reefers. This part of the fuel consumption decreases linearly with the decrease of the number of connected reefers. In total, this figure demonstrates that the propulsion system dominates the shape of the total fuel consumption, while the auxiliary system determining the scope of the total fuel consumption. This conclusion also applies to the low speed operation conditions and the other reference ships.

**Ton-mile Specific Fuel Consumption at Service Speed.** If one neglects the influence of loading fraction on the power requirements of the propulsion system and auxiliary system, a rough estimate can be made that, when sailing at service speed, the ton-mile specific fuel consumption, as well as exhaust emissions, would proportional to the inverse of benefit loading fraction ( $x_b$ ), as shown in Fig. 10.



From Fig. 10, a general conclusion is that the bulk carriers are the most economical ship modes, followed by the container ships. The ferry consumes the most fuel and emits the most exhaust emissions on the ton-mile basis. Meanwhile, Fig. 10 also demonstrates that the larger the ship, the more economical it will be.

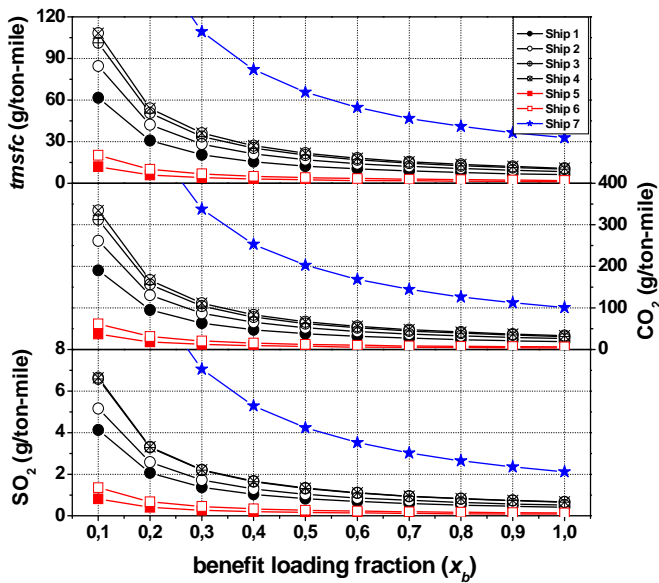


Fig. 10 Estimated fuel consumption and emissions from a rough analysis

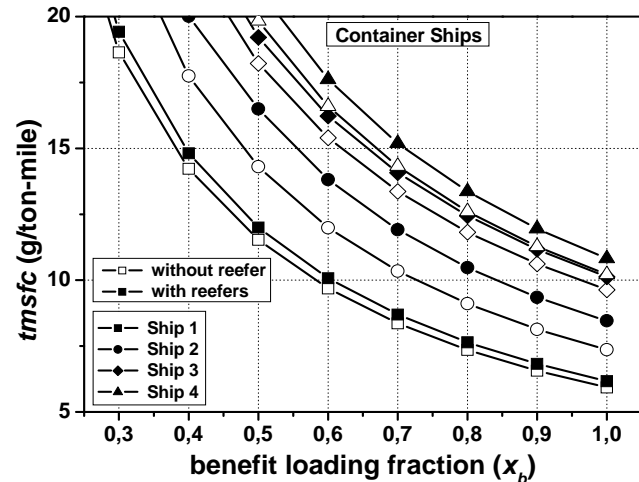


Fig. 11 Ton-mile specific fuel consumptions at service speeds of reference container ships

Concerning the influence of loading fractions, Fig. 11 illustrates the ton-mile specific fuel consumptions in part load conditions of the reference container ships, operated at service speed.

As shown in Fig. 11, for container ships there are two curves indicating the relationships between the ton-mile specific fuel consumption and the benefit loading fraction. For each reference container ship, the lower curve represents the operational

conditions with no reefers on board and the upper one represents those where all of the reefer plugs are used. In other words, the lower one indicates the minimum ton-mile specific fuel consumptions at this speed, while the upper one indicates the maximum values. For other loading strategies, the value of ton-mile specific fuel consumption will be between these two curves.

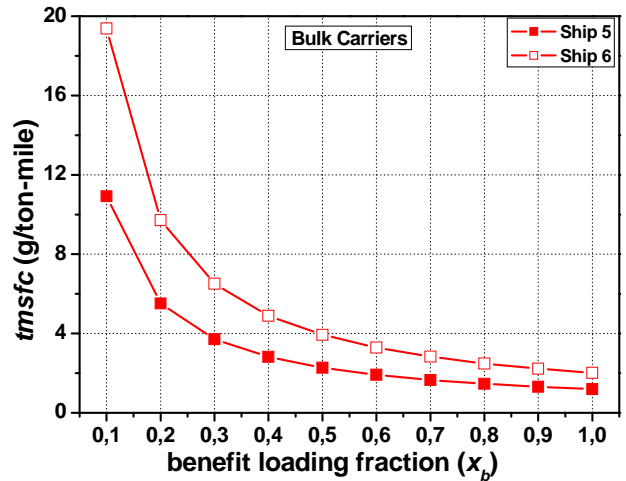


Fig. 12 Ton-mile specific fuel consumptions at service speeds of reference bulk carriers

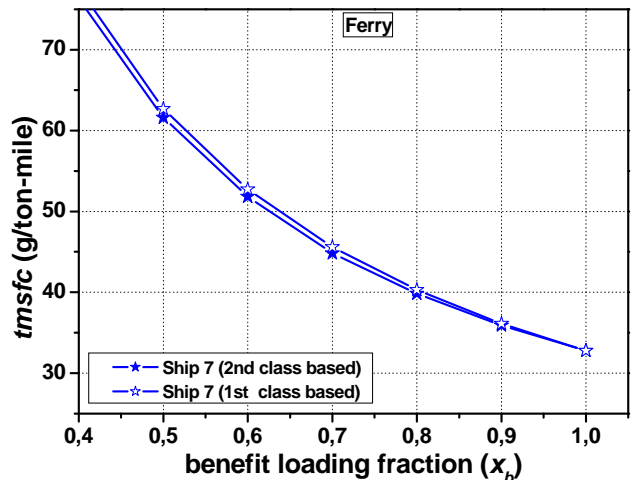


Fig. 13 Ton-mile specific fuel consumptions at service speeds of reference ferry

According to the assumption in this study, for a bulk carrier the consumed power of the auxiliary system remains constant when the loading condition changes. Then, the ton-mile specific fuel consumption of the reference bulk carriers depend only on the amount of cargo and the corresponding propulsion power requirements. As shown in Fig. 12, both of the curves are slightly different from these proportional to the inverse of loading fractions, as shown in Fig. 10.

For the reference ferry, the situation is more complicated compared to those of cargo ships. It is difficult to determine the number of passengers in the 1<sup>st</sup> class and 2<sup>nd</sup> class. Due to the lack of the commercial operation data of this ferry, the same method used in the estimation of container ships is implemented. In Fig. 13, the maximum and minimum ton-mile specific fuel consumptions are indicated by two curves and the results of other loading strategies will be between these two curves.

**Ton-mile Specific Fuel Consumption at Low Speed.** Although the auxiliary power requirements are independent on the sailing speed, it is of importance to consider the ton-mile specific fuel consumptions at low speed, due to the big difference of propulsion power between full load and part load operations at low speed. The results of ship 1 (large container ship) are presented as an example. In order to avoid the influence of the auxiliary system, no reefers are considered in this section.

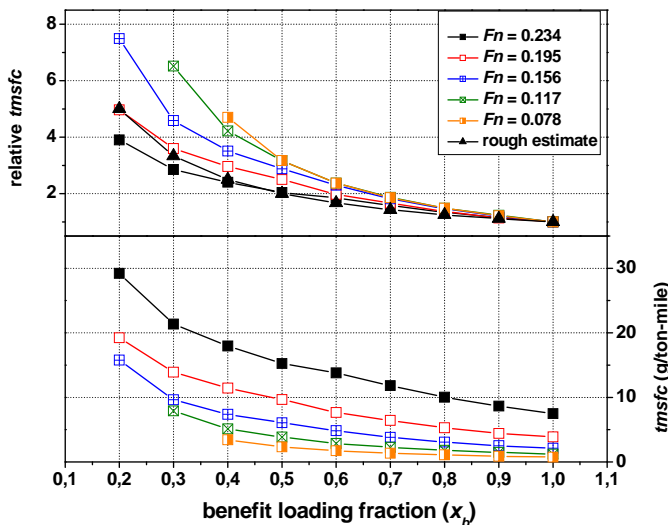


Fig. 14 Ton-mile specific fuel consumptions of Ship 1 at low speeds

Both the absolute and relative values of the ton-mile specific fuel consumption at service speed and low speeds are plotted in Fig. 14. As illustrated in this figure, the ton-mile specific fuel consumption is not only proportional to the inverse of the amount of cargo (determined by the benefit loading fraction), but also depends on the ship speed, which would influence ship resistance. Especially when sailing the ship at low speed with a relative small loading fraction, the influence of loading fraction on ship resistance and therefore the fuel consumption is dramatic. As shown in the figure, the curves of the relative ton-mile specific fuel consumption in low speed conditions are different from the ones calculated by the rough estimate shown in Fig. 10.

## Engine Exhaust Emissions

**Amount of Exhaust Emissions.** In this paper the CO<sub>2</sub> and SO<sub>2</sub> emissions are primarily a function of fuel consumption. But

bearing in mind that the fuels, used in the propulsion system and the auxiliary system, are sometimes different, the influence of the loading fraction on exhaust emissions are related not only to the fuel consumption but also to the fuel properties. Ship 2 (medium container ship), which could carry 48.4% of its total capacity as reefers (990 of 2046), is chosen as an example to present the influence of loading fraction on CO<sub>2</sub> and SO<sub>2</sub> emissions.

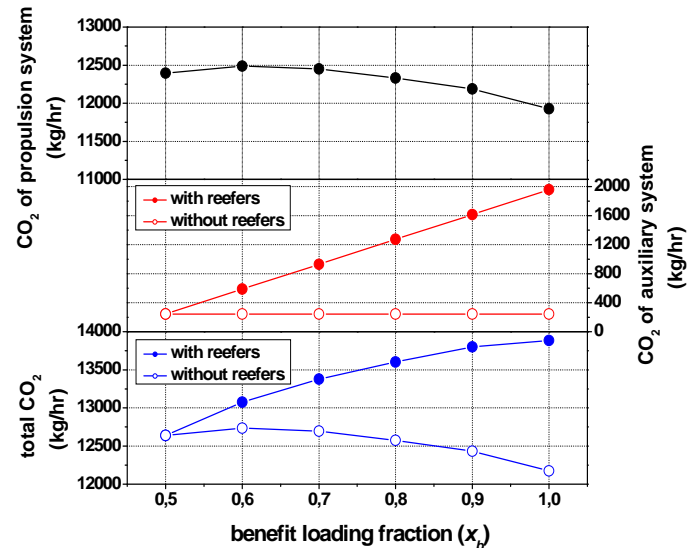


Fig. 15 CO<sub>2</sub> emission of Ship 2 at service speed

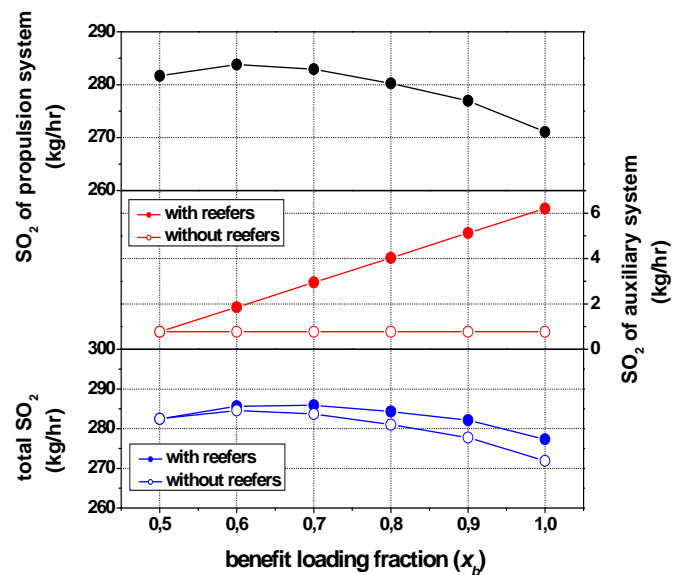


Fig. 16 SO<sub>2</sub> emission of Ship 2 at service speed

At service sailing speed ( $Fn = 0.248$ ), from 50% load to full load, the amounts of CO<sub>2</sub> and SO<sub>2</sub> are plotted separately, yielding the curves of Fig. 15 and Fig. 16.

On the propulsion system side, while the loading fraction decreases, both the CO<sub>2</sub> and SO<sub>2</sub> emissions first go up, until

they reach the maximum value at 60% load, then they decrease. The trend looks the same as that of fuel consumption, shown in Fig. 9.

On the auxiliary system side, the amount of reefers dominates the shape of the curves. The CO<sub>2</sub> and SO<sub>2</sub> emissions will remain constant if there are no reefers in operation. And these emissions increase, when the number of reefers in operation increases.

Due to the fact that the MDO (used in the auxiliary system) contains more carbon but less sulfur than the HFO (used in the propulsion system), the shape of the curve, which indicates the total amount of CO<sub>2</sub> emission, is dominated by the auxiliary system while that of SO<sub>2</sub> emission is dominated by the propulsion system.

**Ton-mile Specific Exhaust Emissions.** When considering the ton-mile specific factors as shown in Fig. 17, the trend of both CO<sub>2</sub> and SO<sub>2</sub> emissions is determined by the amount of the transported cargoes. But, due to the change of ship resistance while sailing the ship at part load conditions, and due to the change of the usage of auxiliary power, the ton-mile specific CO<sub>2</sub> and SO<sub>2</sub> emissions are different from the results of the rough estimate shown in Fig. 10. On the other hand, in every loading condition, the emission values are within the area between the curves, determined by the auxiliary system.

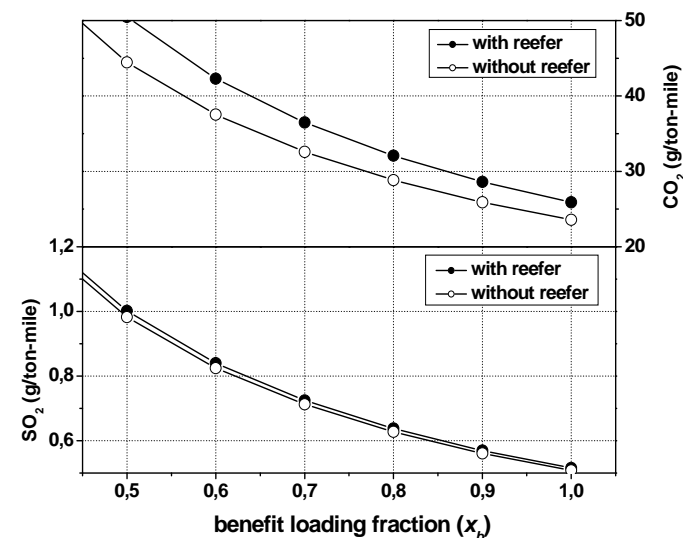


Fig. 17 Ton-mile specific emission factors of Ship 2

## CONCLUSION

As shown in the master equation of ton-mile specific factors, the loading situation (the loading fraction  $x$ ) will influence the fuel consumption and emissions for operational shipping. Part load conditions will change the requirements of both propulsion power and auxiliary power. The values of ton-mile specific factors will be different from the simple theory, in which they are supposed proportional to the inverse of the loading fraction.

The simulation model calculates in what way part load operation conditions will cause changes in ship resistance compared to full load and can accurately predict power and fuel consumption at a particular sailing speed. The assumption of a constant ship resistance factor would cause errors: especially when sailing a ship at low speed with a relative low loading fraction, the error could be dramatic.

In the analysis of exhaust emissions, due to the different properties of fuel oils used in propulsion system and auxiliary system, the influence of loading fraction on CO<sub>2</sub> and SO<sub>2</sub> emissions are different. The influence on auxiliary system load dominates the trend of CO<sub>2</sub> emission, while that on the propulsion system load dominates the trend of SO<sub>2</sub> emission. The results of ton-mile specific emissions demonstrate that, at a particular speed, neglecting the change of the ship resistance in part load conditions would result in a bias of the emission predictions, while the auxiliary system determines the scope of emission situations.

Future research will explore the influence of loading fraction on transient operational conditions, especially in maneuvering.

## REFERENCES

- D. Stapersma, 1994, "The importance of (e) mission profiles for naval ships", *INEC 94 conference*, Plymouth.
- D. W. Taylor, 1943, *The Speed and Power of Ships*, United States government printing office, Washington.
- D.G.M Watson, 1998, *Practical Ship Design*, Elsevier Science.
- D. Stapersma, H.T. Grimmeliuss, 2003, "Trends in propulsion and how they affect environmental sustainability", *RINA 03 conference*, London.
- G. Kuiper, 1992, *The Wageningen Propeller Series*, MARIN Publication 92-001, The Netherlands.
- J. Klein Woud, D. Stapersma, 2002, *Design of propulsion and electric power generation system*, IMarEST Publication, London.
- J. Holtrop, G.G.J. Mennen, 1978, "A statistical power prediction method", *International Shipbuilding Progress*, Vol. 25.
- J. Holtrop, G.G.J. Mennen, 1982, "An approximate power prediction method", *International Shipbuilding Progress*, Vol. 29.
- D. Moor, Patullo, 1968, "The effective horsepower of twin screw ships", BSRA Report 192.
- P. Brussen, 2006, "CO<sub>2</sub>-emissions of various ship types, simulated in an operational year profile", TNO report, 2006-D-R0262.
- R. F. Roddy, 2006, "Neural network predictions of the 4-quadrants Wageningen propeller series", Hydromechanics Department Report, NSWCCD-50-TR-2006/004.

## APPENDIX: Ship data

Refer to (Brussen, 2006)

	SHIP 1	SHIP 2	SHIP 3	SHIP 4	SHIP 5	SHIP 6	SHIP 7
<b>Classification</b>	<b>Large Container ship</b>	<b>Medium Container ship</b>	<b>Container feeder</b>	<b>Coastal feeder</b>	<b>Large Bulk carrier</b>	<b>Medium Bulk carrier</b>	<b>Ferry</b>
<b>Name</b>	Ned Lloyd Southampton	Dole Chile	Jork	Friesedijk	CKS Fortune	Jin Hui	Stena Jutlandica
<b>Dimensions</b>							
Length o.a., [m]	299.9	204.9	157.13	100.8	289	189.99	184.35
Length p.p., [m]	283.8	193.4	147	92.9	279	182	169.05
Beam mld, [m]	42.8	32.24	23.5	15.85	45	32.26	27.8
Draught, [m]	13.5	10.2	8.3	4.88	16.5	10.75	5.8
Depth, [m]	24.4	20.8	12.8	6.18	24.5	16.69	9.4
<i>C<sub>b</sub></i>	0.662	0.649	0.64	0.755	0.84	0.808	0.602
<i>C<sub>w</sub></i>	0.773	0.763	0.756	0.895	0.908	0.884	0.728
<b>Tonnage</b>							
<i>DWT</i> , [ton]	83826	30560	11870	3820	156300	44579	5640
Displacement, [m <sup>3</sup> ]	111825	42540	18903	5585	179250	52559	16903
<b>Machinery</b>							
<b>Main engines</b>							
Install power, [kW]	65880	23920	10920	3280	16858	8203	6480*4
Speed, rpm	100	97	135	750	91	118	550
Fuel type	HFO	HFO	HFO	HFO	HFO	HFO	HFO
<b>Aux engines</b>							
Install power, [kW]	3600*4	3840*3/2880*2	900*2	275*2	750*3	490*3	1760*4
Speed, [rpm]	600	600	900	1500	720	720	750
Fuel type	MDO	MDO	MDO	MDO	HFO	MDO	HFO
<b>Propellers</b>							
Type	Fixed pitch	Fixed pitch	Controllable pitch	Controllable pitch	Fixed pitch	Fixed pitch	Controllable pitch
Diameter, [m]	8.75	6.65	5.1	3.2	8.1	6.35	4.8*2
Speed, [rpm]	100	97	135	184	91	118	150
<b>Speed</b>							
Service speed, [knot]	24.5	21	19	15	15	14	21.5